Available online at www.sciencedirect.com
ScienceDirect
Journal of the European Ceramic Society 28 (2008) 279–288
www.elsevier.com/locate/jeurceramsoc

The effect of mechanical activation on the properties of β-sialon precursors

Małgorzata Sopicka-Lizer[a,*], Marta Tańcula[a], Tomasz Włodek[a], Kinga Rodak[a], Marco Hüller[b], Vladimir Kochnev[c], Elena Fokina[d], Kenneth MacKenzie[e]

[a] *Silesian University of Technology, 40-019 Katowice, Krasińskiego 8, P.O. Box 142, Poland*
[b] *EADS Corporate Research Center, 81663 Munich, Germany*
[c] *Technics and Technology of Disintegration Ltd. (TTD), P.O. Box 432, St. Petersburg 195220, Russia*
[d] *St. Petersburg State University, Institute of Chemistry, Universitetski pr. 26, Petrodvorets, St. Petersburg 198504, Russia*
[e] *School of Chemical and Physical Sciences, Victoria University of Wellington, P.O. Box 600, Wellington, New Zealand*

Received 12 October 2006; received in revised form 26 April 2007; accepted 5 May 2007
Available online 24 July 2007

Abstract

Nanostructured β-sialon precursors were produced from the relevant mixtures of Si_3N_4, AlN and Al_2O_3 by mechanical milling in a new planetary mill with a centrifugal factor of 28 g, at milling times <60 min. Zirconia balls were used in order to avoid the effect of the susceptibility of the separate components to deform under mechanical activation. Several milling regimes were studied and only planetary milling with a high acceleration affected the particles structure. Under these conditions, AlN and Al_2O_3 crystallites were formed with new boundaries and dislocations, but the α-Si_3N_4 particles were more resistant to deformation. Milling at the higher acceleration conditions produces only a small increase in the crystal lattice parameters of the precursor components, but FTIR and ^{27}Al and ^{29}Si solid-state MAS NMR spectroscopy indicates the formation of new tetrahedral AlO_4 units and Si–O–Al bonds, possibly in solid solution or partially reacted hybrid particles of Al_2O_3 and β-Si_3N_4. The total oxygen content in the activated sialon precursor mixture can be limited by replacement of alumina by AlN.

Keywords: Milling; Powders; Nanocomposites; Sialon

1. Introduction

Sialon ceramics (silicon aluminium oxynitrides) are an important class of structural ceramics. Their high toughness and high wear resistance combined with chemical stability offer potential for many commercial applications.[1] Sialons can be produced by the reaction sintering of a mixture containing the appropriate amounts of α-Si_3N_4, AlN, Al_2O_3 and a suitable sintering additive (i.e. Y_2O_3). However, high manufacturing costs hamper the use of these materials in many engineering applications. To obtain the fully dense ceramics with a uniform microstructure pressure assisted sintering is essential because of the low diffusion coefficient of these highly covalently bonded materials and because of the high partial pressure of $Si_{(g)}/SiO_{(g)}$ at temperatures >1500 °C. Thus, if a sufficient amount of sintering additive (i.e. Y_2O_3) is introduced and a homogenous distribution of submicron particles is achieved by slip casting, pressureless sintering at 1750 °C for 6 h yields dense β-sialon ceramic.[2,3]

Wider applications of sialon ceramics in engineering could be achieved if the sintering temperature could be reduced below the temperature at which substantial decomposition of Si_3N_4 occurs, allowing pressure sintering to be avoided. This might be achieved by the use of submicron or nanometer-sized powders because the sintering of a ceramic powder compact is driven by a reduction in the surface area and the curvature of the necks between the grains. A previous report showed that the densification at 1500 °C of plasma-chemical synthesized sialon nano-powder with a specific surface area of 65 $m^2\ g^{-1}$ resulted in a density of 96%.[4] However, plasma-chemical synthesis in a nitrogen plasma would increase the cost of the initial powder significantly. Increasing interest in nanostructured powders has resulted in the development of alternative preparation strategies, namely by a top-to-bottom process using high-energy milling.[5,6]

* Corresponding author. Tel.: +48 326034476; fax: +48 326034400.
E-mail address: malgorzata.sopicka-lizer@polsl.pl (M. Sopicka-Lizer).

0955-2219/$ – see front matter © 2007 Elsevier Ltd. All rights reserved.
doi:10.1016/j.jeurceramsoc.2007.05.003

This process involves a large number of collisions between the particles, the milling media and the walls of the working chamber of the planetary mill. The outcome is not only particle size reduction but also the formation of defects in the crystalline lattice, structural transformations, phase transitions and chemical reactions. If the applied energy density is similar to the energy of crystal formation then the destruction of long-range atomic ordering can proceed effectively.[7] The formation of structural defects will introduce enhanced diffusivity, allowing the compound to nucleate and grow at a relatively low temperature for that particular material. Mechanochemical synthesis of mixed oxides with ionic bonds from carbonates with low lattice energy is well known.[8] The availability of new planetary mills with higher acceleration and higher energy densities has enabled mechanical activation of more covalently bonded compounds with higher lattice energy such as mullite,[9] alumina and quartz.[10]

Recent reports have shown that mechanochemical activation can be applied to compounds such as sialons, in which mixtures of the component nitrides and hydroxides, when milled in a planetary mill at 400 rpm for 48 h and subsequently heated at 1600 °C form a variety of sialon products.[11] On the other hand, a mixture of halloysite and fine carbon powder after similar mechanochemical activation was exposed to carbothermal reduction, resulting in the formation of the expected sialon products in the temperature range 1200–1400 °C.[12] Milling at 475 rpm of a low z-value sialon precursor mixture[13] and of β-Si_3N_4 with alumina and yttria sintering additives[14] resulted in a non-equilibrium amorphous phase containing many well-dispersed nanocrystalline β-Si_3N_4 particles[14] which could be consolidated to a fully dense ceramic by spark plasma sintering at 1550–1600 °C for 5 min.

However, the use of high ball-to-powder ratios (20:1[14] or even 50:1[11]) combined with very long milling times (48 h[11] or 4 h[14]) must lead to the wearing of the milling balls themselves. If the milling medium is of the same phase composition as the milled powder, then the source of the resultant amorphous powder cannot be distinguished. Thus, it is difficult to prove that the nanocrystalline β-Si_3N_4 particles observed by Xu et al.[14] resulted from the original particles and not from the milling media debris. Another question arising in mechanochemical studies of sialon precursors relates to the different susceptibility to mechanochemical amorphization of the components of the mixture. It has been shown that milling periclase for a certain time reduces the size of the crystallites to 15 nm, whereas the same milling conditions reduce the size of corundum to 31 nm and quartz to 65 nm.[10]

In order to further explore the mechanical activation of sialon precursors, the susceptibility to deformation under high-energy planetary milling of the components, especially silicon nitride, must be examined. Such a study would be facilitated by the use of a mill with higher acceleration, allowing shorter milling times to be used. Furthermore, for the reasons discussed above, the milling balls must be made from a different material to the milled powder. Such facilities are available at Technics and Technology of Disintegration Ltd. (TTD, Russia) where a new planetary mill capable of acceleration up to 65 g has been built. The aim of the present study is to show the influence of the milling acceleration (i.e. energy) on the properties of the sialon precursors. A detailed study of the powder properties after milling at accelerations of 4.2 g and 28 g for various times was made with the aim of determining whether silicon nitride can be converted into nanostructured powder if sufficient milling energy density can be supplied. These conditions may even lead to the formation of a silicon nitride solid solution. A further set of experiments was carried out on mixtures without oxides, to shed light on the problem of nitride oxidation during milling.

2. Experimental procedure

The initial materials were commercial Si_3N_4 (H.C. Starck—B7), AlN (H.C. Starck—C), and α-Al_2O_3 prepared from $Al(OH)_3$ by firing at 1200 °C (total contaminants 0.2 wt%, $d_{50} = 16\ \mu m$). The silicon nitride powder contained 85–90 wt% of the α form and 10–15 wt% of β-Si_3N_4. The specific surface areas of nitrides were about 5 $m^2\ g^{-1}$ and that of α-Al_2O_3 was 0.8 $m^2\ g^{-1}$. One mixture for milling (mixture 1) contained 49.5 wt% of Si_3N_4 + 36 wt% of α-Al_2O_3 + 14.5 wt% of AlN, corresponding to the β-sialon composition $Si_3Al_3O_3N_5$ where $z = 3$. Another mixture (mixture 2), which did not contain alumina, consisted of 49.5 wt% of Si_3N_4 + 50.5 wt% of AlN.

Milling was carried out in planetary mills, for which the centrifugal factor (acceleration, non-dimensional value) is given by:

$$\Phi = \frac{R\Omega^2}{g}, \tag{1}$$

where R is the distance between the centers of the rotor and the drum (m), Ω the angular velocity of the rotor rotation (s^{-1}), g is the acceleration due to gravity ($m\ s^{-2}$).

Mixing and milling was carried out using the following milling equipment:

- a roller bench with 5 mm silicon nitride balls in isopropanol for 24 h (resulting samples designated RB),
- an attritor (Model 01STD, Union Process) with 5 mm silicon nitride balls in isopropanol and balls-to-powder ratio 6:1 with a rotational speed of 60 rpm (resulting samples designated AT),
- a planetary mill (Model Pulverisette 6, FRITSCH) with 20 mm hardened steel balls, ball-to-powder ratio 20:1 with a rotational speed of 250 rpm. This mill had an acceleration of 4.2 g and the milling was carried out in an argon atmosphere for 30–120 min. To minimize the temperature rise in the milling vial, the milling process was carried out for periods of 15 min, interspersed with rest periods of 15 min. The maximum milling time was 120 min. Iron contamination increased rapidly at longer milling times because of the relatively high ball/powder ratio. The resulting samples are designated PM,
- a planetary mill built by TTD, providing an acceleration of 28 g. The powder was milled with zirconia balls and a powder-to-ball ratio 12:1 for 21; 33 and 45 min. The aluminium-nitride-based mixture 3zN was milled for only

45 min, with silicon nitride balls. The rotor rotation rate was 422 rpm with a jar rotation rate of 920 rpm, resulting in a value of the centrifugal acceleration of 28 g. The resulting samples are designated MPL.

The milled sample powders were characterized by their BET specific surface areas. The total pore volume and the average pore diameter were derived from the nitrogen adsorption/desorption isotherm by the single point method (model 2010, ASAP). The densities of the activated powders were measured by helium picnometry (AccuPyc 1330) and the particle size distribution was determined by laser diffraction (Fritsch, Analysette 22) on powder samples suspended in distilled water and ultrasonically treated for several minutes. The particle size distribution was recorded both at the beginning of a measurement and after ultrasonic treatment. Subsequently the ultrasonic treatment was repeated and the particle size distribution was redetermined until no further changes were observed in the particle behaviour. XRD measurements were performed in the 10–90° 2θ range with Cu Kα radiation and an incident beam monochromator (X'pert, Philips-Panalytical). A Retvield refinement was applied to the XRD results from a continuous step scan (0.0080° 2θ step size and 957.6 s scan time) to calculate the phase composition, crystallite size, unit cell parameters and the crystallite micro-strain. FTIR spectroscopy (Model FTS-60v, Bio-RAD spectrometer) was carried out on both the starting mixtures and the activated powders. The FTIR spectra were recorded in the range 400–4000 cm^{-1} on samples suspended in KBr pellets. The nitrogen and oxygen contents were measured by infrared analysis of CO produced by hot-gas extraction (ELTRA ON). Specimens for TEM were carbon coated and observed in a JEOL model 100B transmission electron microscope at an accelerating voltage of 100 kV. Electron diffraction was measured by the means of selected area diffraction (SAD) and the patterns were resolved with the use of the ELDYF program.

^{27}Al and ^{29}Si MAS NMR spectroscopy was carried out at a field of 11.7 T using a Varian Unity 500 spectrometer and Doty MAS probes spun at 4 MHz for Si and 6 MHz for Al. The ^{27}Al spectra were acquired using a 15° pulse of 1 μs with a 1s recycle delay, the spectra referenced to $Al(H_2O)_6^{3+}$. The ^{29}Si spectra were acquired with a 90° pulse of 60 μs with a recycle delay of 100 s, the spectra referenced to tetramethylsilane (TMS).

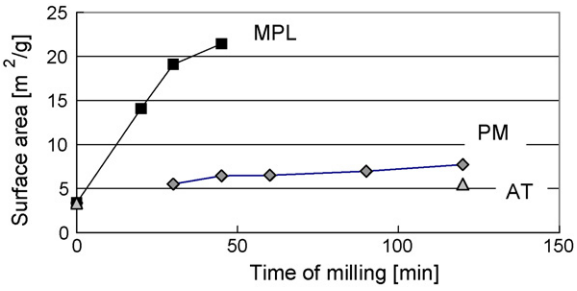

Fig. 1. Specific surface area of sialon precursor mixture 1 after milling for various times in different mills with various centrifugal factors. Key: (■) MPL mill 28 g, (◊) PM mill, 4.2 g, (△) attritor.

3. Results and discussion

3.1. Effect of milling on the particle characteristics

Fig. 1 presents the specific surface areas of the powders milled for various times and in different mills. Attrition milling was the least effective method of reducing the particle size increasing the surface area of the particles. The use of the planetary mill with 4.2 g acceleration does not increase significantly the surface area of the powder mixture, but the milling time is shortened by comparison with attrition milling. It can clearly be seen that longer milling times with 4.2 g acceleration lead to slow but steady increase of the powder surface area. However, the process is dramatically speeded up under higher energy milling conditions and a significantly higher powder specific surface area is observed after 20–45 min of milling at 28 g (Fig. 1).

The particle size distribution of the mixtures after treatment in the planetary mill at 28 g was recorded as the volume percentage of particles determined in water, indicating that the polar environment of the water enhances the formation of agglomerates, evidenced by an increased number of large particle-like structures occurring in the size range 20–100 μm. Longer milling times at 28 g (MPL samples) produced more large particles (Fig. 2). Ultrasonic treatment of the suspension broke up a significant number of the agglomerates, but not all of them disintegrated, leading to the observation of an increase in the diameter d_{50} diameter after longer milling times. These results are summarized in Table 1.

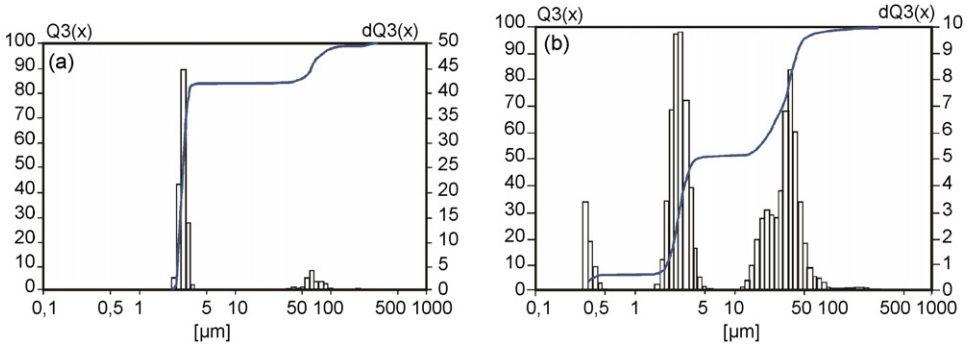

Fig. 2. Particle size distribution of the sialon precursor mixture 1 after milling in the MPL mill at 28 g for (a) 21 min and (b) 45 min. The samples were not subjected to ultrasonic treatment before the measurement.

Table 1
Characterization of the sialon precursor powders after milling in the MPL planetary mill with an acceleration of 28 g

Milling time (min)	Unmilled	21	33	45
d_{BET} (μm)	0.508	0.122	0.090	0.080
d_{50} after milling (μm)		3.59	7.14	16.32
d_{50} after milling + ultrasonic treatment (μm)		2.89	2.74	4.04
Porosity (vol.%)	9.4	14.96		16.73
Pore mean diameter (nm)	12.9	14.6		8.44

The d_{BET} results are from nitrogen adsorption/desorption and the d_{50} results were determined by laser diffraction.

The formation of agglomerates was less pronounced in samples milled in the PM mill at 4.2 g acceleration. Milling for 30–90 min gave a tri-modal distribution with the first maximum at about 0.35 μm being observed after the first 30 min of milling. The d_{50} diameter of the particles in the suspension without ultrasonic treatment changed from 3.9 μm (after milling for 30 min) to 4.84 μm (after milling for 60 min), to 4.66 (after milling for 90 min) and finally to 12.99 μm (after milling for 120 min). Thus, the mean diameter d_{50} of the measured particles was similar to that of the samples milled at higher acceleration. In both cases, ultrasonic treatment broke up the weaker agglomerates

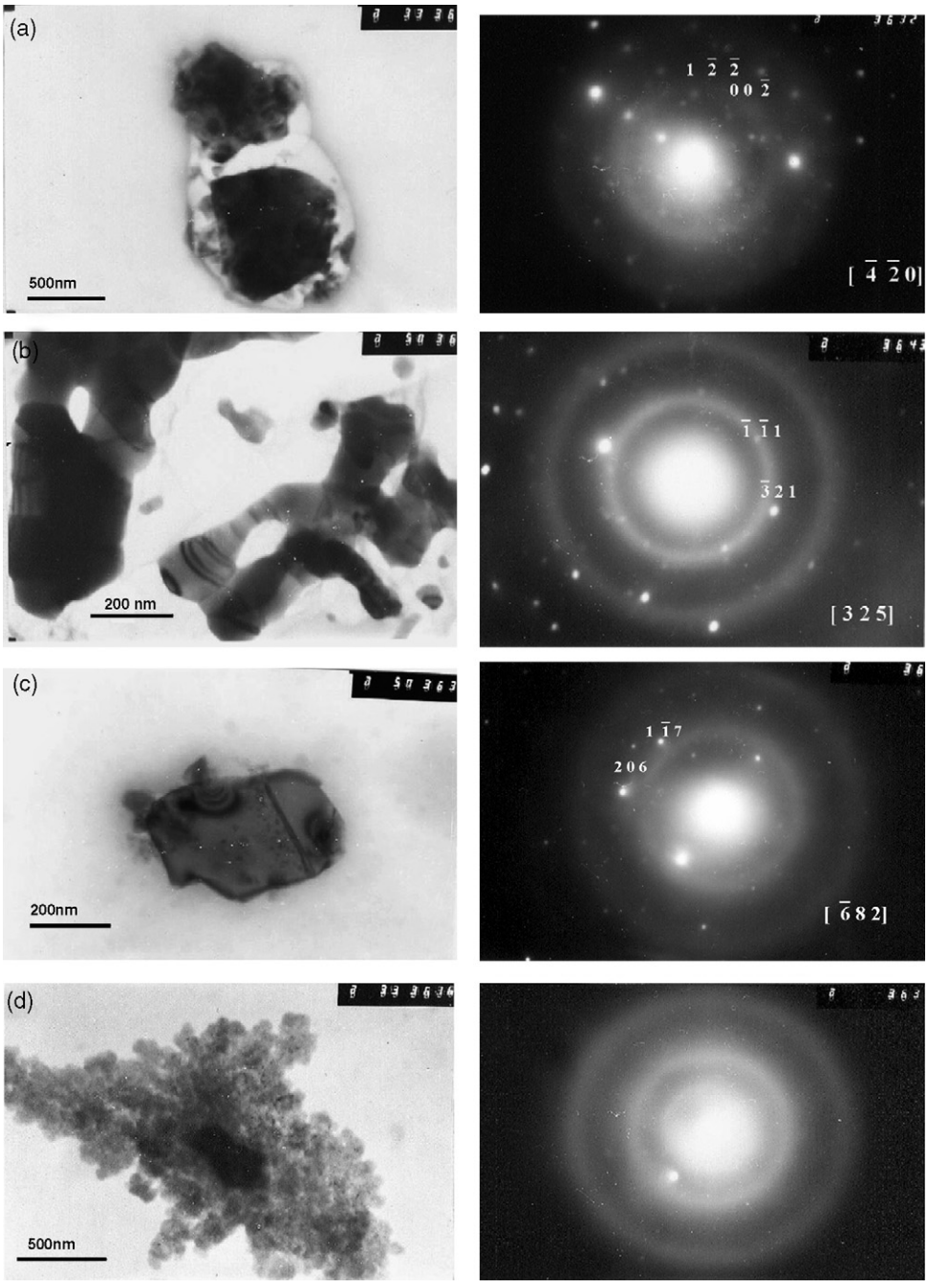

Fig. 3. TEM micrograph and electron diffraction patterns of the powder particles in mixture 1 after milling at 28 g acceleration for 45 min in the MPL mill. Key: (a) α-Si_3N_4, (b) β-Si_3N_4, (c) α-Al_2O_3, and (d) unidentified particle.

Table 2
XRD Phase composition of the sialon precursor mixtures before and after milling in planetary mills with various accelerations

	Mixture				
	1	1	1	2	2
Mill type	RB	PM (4.2 g)	MPL (28 g)	RB	MPL (28 g)
Milling medium	Si_3N_4	Steel	ZrO_2	Si_3N_4	Si_3N_4
Milling time (min)	–	120	45	–	45
Phase composition (wt.%)					
Al_2O_3	32.1	33.1	47.5	0	0
α-Si_3N_4	45.3	44.3	34.1	45.5	42.9
β-Si_3N_4	7.8	8.2	3.5	3.9	7.7
AlN	14.8	14.4	6.4	50.6	49.4
ZrO_2	0	0	8.4	0	0

into structures with diameters of 2–3 μm while the volume fraction of the first maximum (0.35 μm) was less apparent.

Calculation of the mean particle diameter from the BET data shows a discrepancy between the values of d_{BET} from the specific surface area and the average particle size d_{50} from the laser diffraction measurements (Table 1). As discussed above, the reason for the observed high values of d_{50} could be the formation of agglomerates. The discrepancy could also be caused by the surface porosity of the particles; a similar inconsistency between the laser diffraction results and the calculated BET diameters of the particles was also observed in the initial powders. The calculated d_{BET} values of the particles after milling at 4.2 g acceleration did not change significantly with milling time, being 0.31 μm after milling for 30 min and 0.22 μm after milling for 120 min. Milling at higher acceleration (28 g) produced a large discrepancy between the values from the BET specific surface area and those measured by laser diffraction (d_{50}), this discrepancy increasing with increased milling time. The porosity measurements (Table 1) confirm the increase of particle porosity after milling at 28 g acceleration. The particle diameters d_{BET} after milling at 28 g for 33 and 45 min are in the nanoscale range (90 and 80 nm, respectively).

TEM observation confirms the presence of defects in the particles after milling at 28 g acceleration, and the fact that the diameter of the particles is <1 μm (Fig. 3). The particles are damaged and porous (Fig. 3b), consistent with the porosity measurements, suggesting that micro-strains are present in the crystalline lattice (Fig. 3b and c). Some of the particles have an amorphous appearance (Fig. 3d). No AlN particles could be identified by electron diffraction but the highly defective, amorphous particles (Fig. 3d) are assumed to be AlN-derived. Electron diffraction shows that the most defective particles were those of alumina whereas the α-Si_3N_4 particles appear to be almost undamaged. It is clear that milling in the planetary mill produced limited diminution of the powder particles but caused significant distortion of their crystal lattice.

3.2. XRD characterization of the milled precursors

Rietveld refinement of the XRD data made it possible to distinguish between different modes of behaviour of the particles after milling in the planetary mill. XRD shows the presence of ZrO_2 after milling in the MPL planetary mill with zirconia balls, the amount of ZrO_2 increasing with milling time. The use of zirconia balls ensures that the observed changes in the silicon nitride particles were induced by the planetary milling itself since there was no Si_3N_4 debris from the milling media. However, the weight fraction of zirconia in the sample after 45 min milling was unexpectedly large (Table 2).

Changes in the phase composition showed that oxidation of the nitrides took place during milling, evidenced by the increase of α-Al_2O_3 content and the decrease of the nitride weight fraction (Table 2). The most significant oxidation was observed for AlN, of which nearly 50% of the initial content appears to have been converted to alumina by milling. The resulting increase in alumina content and decrease in silicon nitride was confirmed by the measured nitrogen content of the mixtures after milling (Fig. 4). Milling of the nitrides in the mixture results in the formation of fresh surfaces and their subsequent oxidation produces surface alumina on the AlN particles and amorphous silica on

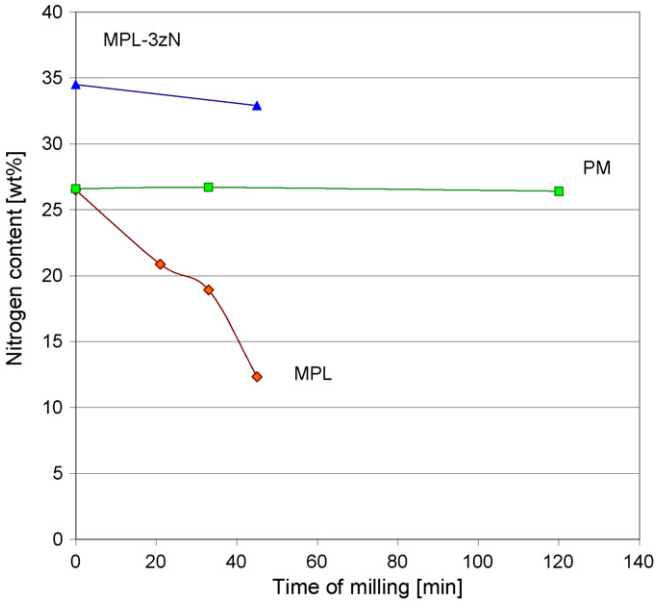

Fig. 4. Nitrogen content of the sialon precursor mixtures as a function of milling time. Key: (■) mixture 1 milled at 4.2 g acceleration in PM mill, (♦) mixture 1 milled at 28 g acceleration in MPL mill, (▲) mixture 2 milled at 28 g acceleration in MPL mill.

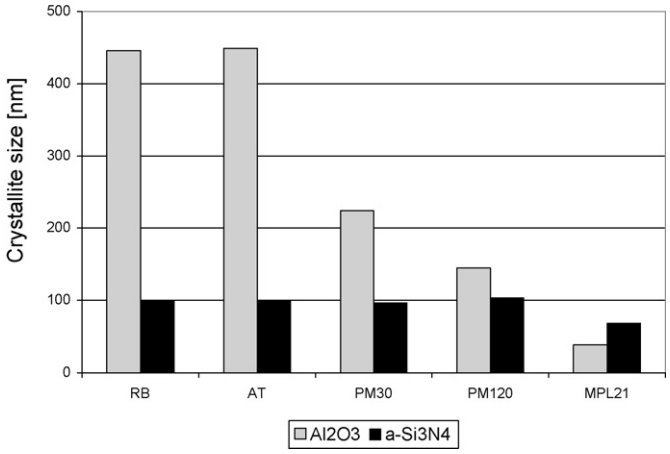

Fig. 5. Crystallite size of alumina and α-Si_3N_4 in mixture 1 and after initial mixing (RB) and milling in the attritor (AT), in the PM mill at an acceleration of 4.2 g and the MPL mill at an acceleration of 28 g. The milling times (min) are indicated after the mill designation.

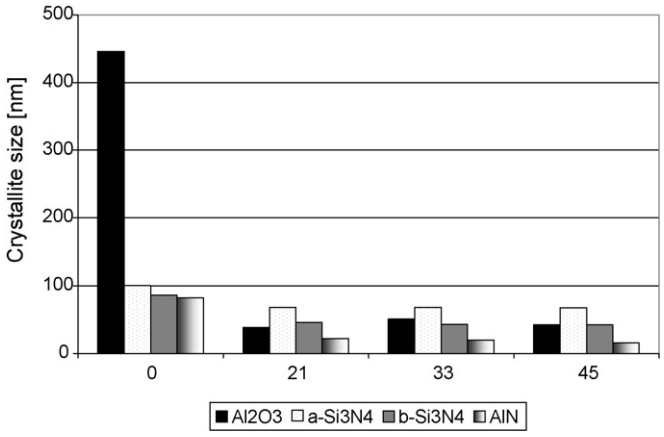

Fig. 6. Crystallite size of the sialon mixture 1 constituents after milling for the indicated times at 28 g acceleration in the MPL mill.

the silicon nitride. However, a decrease in the nitrogen content to such an extent could be a serious drawback to this particular milling procedure. Some of the oxygen comes from the zirconia debris, but another reason for the high degree of AlN oxidation is its affinity for water or water vapour. Since the powders were not dried prior to milling, their residual humidity could enhance AlN oxidation during milling. On the other hand, since amorphous silica was not detected by XRD, the increase of alumina may be an artifact. This possibility was confirmed by milling mixture 2 (without alumina) in the MPL mill with silicon nitride balls. In this case no alumina was found after milling for 45 min (Table 2). The higher amount of β-Si_3N_4 by comparison with the initial composition could result from the wear of the silicon nitride milling media. The nitrogen content was maintained at a reasonable level (Fig. 4), demonstrating that sialon precursors can be activated in a planetary mill with high acceleration.

The effect of planetary milling on the structure of the particles is shown by the XRD crystallite size after milling (Fig. 5). As expected, attrition milling did not change the crystallite size of any of the components and the increase of the surface area was due only to diminution because of wear. Because the alumina particles in the initial mixture were considerably larger than the nitride particles, the increase in the surface area after milling in the attritor was expected to be due to diminution of the alumina particles. Planetary milling at lower acceleration produced a reduction of the crystallite size, especially of the alumina particles. Milling at higher energy (28 g acceleration) for only 21 min resulted in lower crystallite sizes of both the alumina and silicon nitride, with values of the crystallite sizes in the nanoscale range (Fig. 5). TEM observation confirmed the presence of defective alumina particles and microstrain formation (Fig. 3c), with new dislocations and broken alumina particles visible.

The susceptibility of silicon nitride to deformation under planetary milling conditions is less pronounced and can be observed only after high-energy milling (Fig. 5). Fig. 6 shows that α-Si_3N_4 is the most resistant compound to deformation under planetary milling and increasing the milling time does not increase its susceptibility. By contrast, β-Si_3N_4 particles with dislocations were observed by TEM (Fig. 3c). It seems that only milling with higher energy results in structural damage of that compound. The destruction of AlN particles after high-energy planetary milling is the most effective, producing particles of 30 nm average crystallite size. These results are consistent with the TEM study (Fig. 3d).

An interesting question is whether high-energy milling of these mixtures can induce chemical reactions or form solid solutions. In an attempt to examine this question, the lattice constants of the activated compounds were compared (Table 3), but the difference between the lattice parameters of the milled and unmilled are very small (<0.01%). Such a subtle increase in the parameters suggests an exchange of ions rather than formation of crystallite micro-strain. Milling-induced chemical reactions between the components were therefore examined by spectroscopic techniques (FTIR and solid-state MAS NMR).

3.3. Spectroscopic examination of the milled precursors

FTIR and solid-state MAS NMR was used to examine the possibility of bond formation in the milled sialon precursor mixtures. FTIR spectra were obtained for the initial mixture and after milling at 28 g acceleration for 21–45 min. For comparison, the FTIR spectra were also obtained for each component separately. The absorption bands in the initial compounds and in the initial mixture are listed in Table 4

Table 3
Lattice constants and crystallite strain of sialon precursor (mixture 1) unmilled but mixed (sample RB) and after activation at 28 g for 45 min (sample MPL 45)

Sample	Phase	*a* (Å)	*c* (Å)	Strain (%)
Unmilled	α-Si_3N_4	7.7517	5.6193	0.067
Unmilled	β-Si_3N_4	7.6062	2.9081	0.158
Unmilled	Al_2O_3	4.7586	12.9896	–
Unmilled	AlN	3.1111	4.98	0.109
Milled	α-Si_3N_4	7.7524	5.6198	0.034
Milled	β-Si_3N_4	7.6034	2.9101	0.221
Milled	Al_2O_3	4.7605	12.9922	0.092
Milled	AlN	3.1116	4.9825	0.001

Table 4
Literature positions of the FTIR absorption bands of AlN, α-Al_2O_3, α-Si_3N_4 and β-Si_3N_4 compared with the present non-activated mixture 1(RB)[21]

Wavenumbers (cm^{-1})					Assignment	Reference
AlN	Al_2O_3	α-Si_3N_4	β-Si_3N_4	Mixture 1		
		1034	1037	1034	SiN_4	[15]
				1021	SiN_4	[15]
		954		956	$OSiN_3$	[15]
			949	944	Si-N	[20]
		935		937	[SiN_4]	[15]
		918	918	915	Si-N	[15]
		906		907	Si-N	[15]
		893		894	Si-O	[15]
		872		872	Si-N	[15]
		854		855	Si-N	[15]
800-600	656	684		685	Al-N	[15], [17]
				652	Al-O	[15]
				648	Al-N	
	603			616	[AlO_6]	[19]
		600		601	[Si_2ON_2]	[15]
		578	580			
	559			583	Al-O	[15]
	501			510	Al-O	[21]
		495	497	495	[Si-O]	[15]
	466	461		462	[AlO_6]	[16]
	463	443	445		Si-O	[15]
	414	410		411	Al-O Si-N	

and the spectrum of the mixture milled for 21 min is shown in Fig. 7. Figs. 8 and 9 show these spectra and the difference spectra in the region of aluminium–oxygen/nitrogen and silicon–oxygen/nitrogen vibrational bands, respectively.

The strongest band in the 400–700 cm^{-1} region contains mainly contributions from Al–O and Al–N absorptions, whereas the 495 cm^{-1} and 601 cm^{-1} peaks are due to Si–O vibrations (Si_2ON_2 group), according to Antsiferov et al.[15] The absorption bands at 462 and 616 cm^{-1} (Fig. 7) correspond to Al–O vibrations of the [AlO_6] octahedra[16] while the peaks at about 648 and 685 cm^{-1} are attributed to the A_1 and E_1 IR-active modes of AlN.[15,17]

The effect of high-energy milling on the FTIR spectrum of the mixture can clearly be seen in Fig. 8, in which the new absorption band at 474 cm^{-1} corresponds to a Zr–O

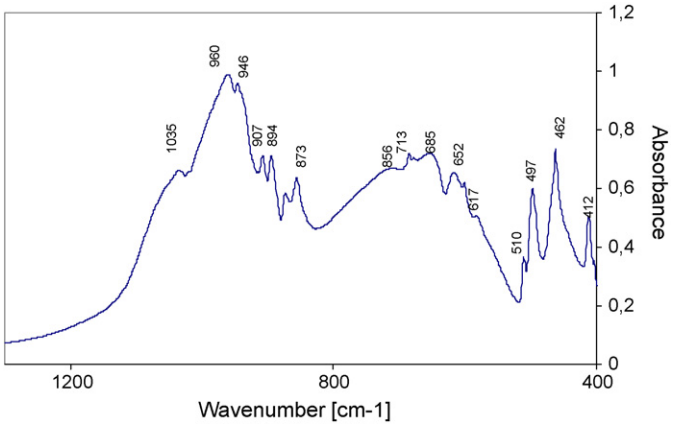

Fig. 7. FTIR absorbance spectrum of sialon precursor mixture 1 after milling for 21 min at 28 g acceleration in the MPL mill.

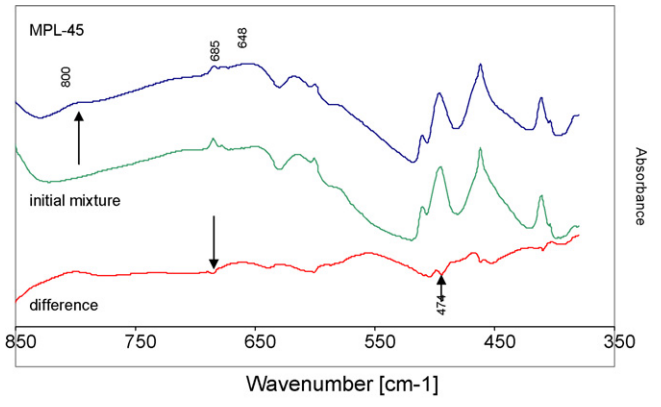

Fig. 8. FTIR absorbance spectra in the region 850–400 cm^{-1} of sialon precursor mixture 1 before milling (RB) and after milling for 45 min at 28 g acceleration in the MPL mill (MPL-45). The difference between the two spectra is shown at the bottom of the figure.

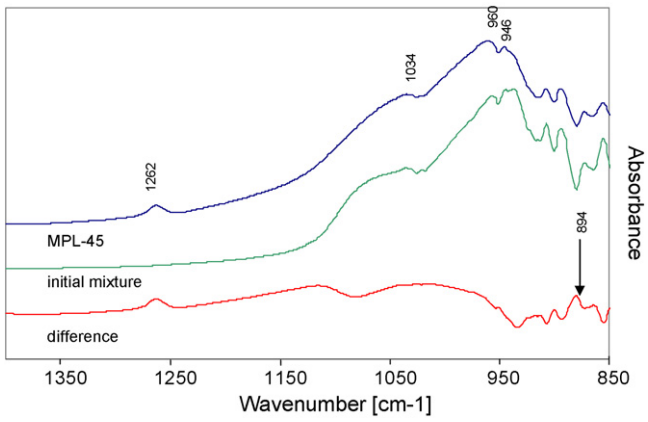

Fig. 9. FTIR absorbance spectra in the region 800–1300 cm^{-1} of sialon precursor mixture 1 before milling (RB) and after milling for 45 min at 28 g acceleration in the MPL mill (MPL-45). The difference between the two spectra is shown at the bottom of the figure.

vibration[18] from the milling ball debris. The most significant changes induced by high-energy milling are visible in the Al–N region (685–648 cm^{-1}) and six-fold coordinated aluminium (462 cm^{-1}). The peaks corresponding to the Al–N vibrations are broadened and their intensity decreases, consistent with the XRD findings of partial oxidation of AlN and crystalline lattice deformation. The shoulder at about 800 cm^{-1} in the spectrum of the milled powder has been attributed to tetrahedral [AlO_4] units.[19] Four-fold coordinated Al occurs in the transition aluminas or in sialons where a Si–N pair is replaced by Al–O. Transition alumina is a less likely product of AlN oxidation during milling, and, furthermore, peaks centered at 810, 814 or 800 cm^{-1} are found in β-sialon, X-sialon and 15-R phase, respectively.[15] The appearance of this shoulder in the powder obtained after 45 min milling is probably due to the replacement of Si–N bonds by Al–O in the β-Si_3N_4 lattice by reaction with Al_2O_3 during high-energy milling.

The spectra of the powder before and after milling for 45 min in the 800–1300 cm^{-1} region (Fig. 9) shows a strong band at 850–1100 cm^{-1}, containing contributions from the Si–N and Si–O stretching vibrations.[20] The 956 cm^{-1} peak corresponds to $OSiN_3$ groups.[15] Remarkable changes occur in the absorption bands in this region after milling for >21 min. The intensity of the broad band at 950 cm^{-1} increases, with a simultaneous decrease in the 946 cm^{-1} band. This behaviour is exaggerated by the greater contribution from the oxygen vibration, possibly resulting from the presence of Al–O in the β-Si_3N_4 lattice as well as from the amorphous silica layer growing on the surface of the Si_3N_4 particles. The subtle increase observed in the 894 cm^{-1} peak of the milled specimens corresponds to the Si–O vibrations.[15]

The band at about 1040 cm^{-1} indicates the existence of [SiN_4] tetrahedra in the silicon nitride lattice,[15] and shifts to higher wave numbers after mechanical treatment. This shift arises from an increased oxygen contribution to the [SiN_4] tetrahedra because of the replacement of nitrogen by oxygen in the lattice of Si_3N_4 and the formation of Si–O–N bonds. One further peak at 1262 cm^{-1} in the spectrum of the specimens milled for 45 min is outside the region of the IR-active Si–O and Si–N bonds and has been ascribed[20] to N–O bonds, although this peak has not been reported in the IR spectrum of sialons.[15] Nevertheless, changes in the FTIR spectra induced by high-energy milling

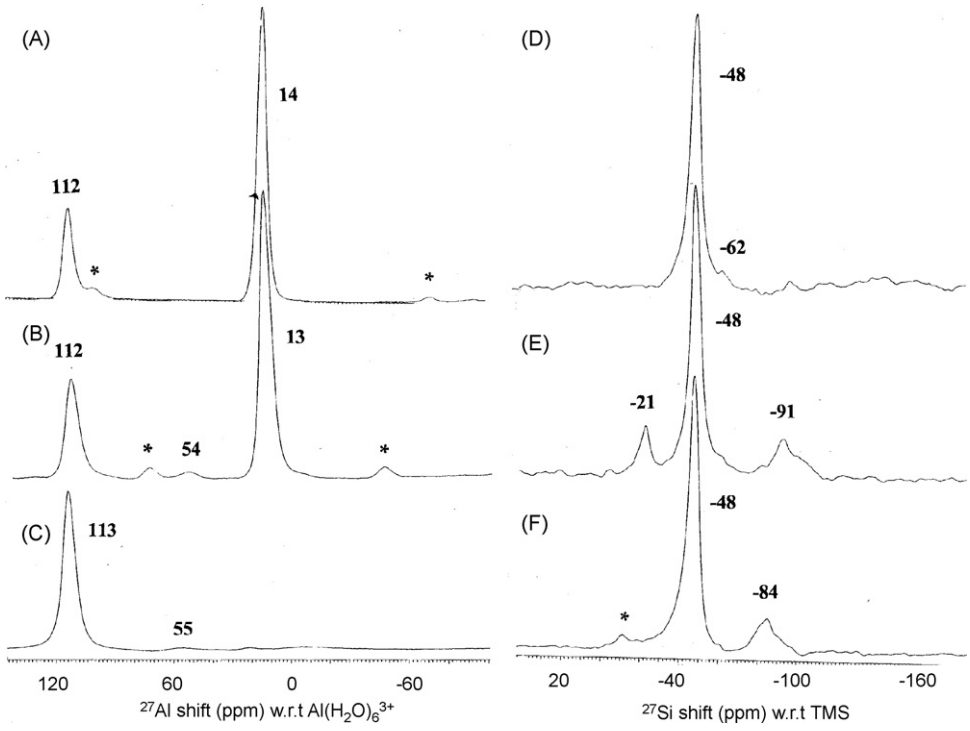

Fig. 10. 11.7 T solid-state MAS NMR spectra of sialon precursor mixtures, unmilled and milled at 28 g acceleration in the MPL mill. (A–C) ^{27}Al spectra, (D–F) ^{29}Si spectra. Asterisks denote spinning side bands. (A and D) Unmilled starting mixture 1. (B and E) Mixture 1 milled for 45 min. (C and F) Mixture 2 milled for 60 min.

depend on the milling time. Some of these changes, including the intensity decrease and broadening of the Al–N band at 685 cm^{-1} and the Si–N stretching vibrations at 854 and 872 cm^{-1} are seen in all the milled specimens, but especially after longer milling times. However, changes in bands related to the vibrations of [SiN_4] tetrahedra at 1034 cm^{-1}, the shoulder at 800 cm^{-1} and the new band at 1262 cm^{-1}, were observable only in the FTIR spectrum of the specimen milled for 45 min. It appears that the formation of a β-Si_3N_4 solid solution takes place during milling but nanocrystalline, amorphous particles derived from AlN are probably implicated in the process.

The ^{27}Al and ^{29}Si MAS NMR spectra of the unmilled and milled precursor mixtures are shown in Fig. 10. Before milling, mixture 1 shows the expected ^{27}Al resonances of AlN and Al_2O_3 at 112 and 14 ppm, respectively (Fig. 10A) and the ^{29}Si resonance of Si_3N_4 at −48 ppm (Fig. 10D). The small ^{29}Si peak at −62 ppm indicates the presence of a trace of Si_2N_2O impurity.[22] Milling this sample in the MPL mill for 45 min at 28 g with ZrO_2 balls produces a small new ^{27}Al resonance at 54 ppm (Fig. 10B) corresponding to the formation of tetrahedral AlO_4,[22] and two new ^{29}Si resonances (Fig. 10E). The broad ^{29}Si feature at −91 ppm suggests the formation of new Al–O–Si bonds, as previously observed when mixtures of alumina and silica are mechanochemically treated,[23,24] while the new peak at −21 ppm is in the Si–C region[22] and may arise from milling debris. Milling of mixture 2 (without Al_2O_3) for 60 min at 28 g produces a similar ^{27}Al resonance (Fig. 10C), but without the Al_2O_3 resonance at 14 ppm and with a less intense AlO_4 feature at 55 ppm. The ^{29}Si spectrum of this sample (Fig. 10F) shows a significant Al–O–Si resonance at −84 ppm, indicating that this new unit is formed by oxidation of the nitrides and the reaction between them. Thus, the MAS NMR spectra confirm and complement the findings of the other techniques used in this study.

4. Summary

This work shows that high-energy planetary milling of sialon precursor mixtures (nitrides and oxides) produces significant damage to the crystalline lattices of the components after milling for <1 h. The extent of the damage varies for the different starting compounds and depends on the applied milling energy. Milling at 4.2 g acceleration in a PM mill did not damage the silicon nitride particles but the particles of alumina and aluminium nitride particles were reduced to smaller crystallites. Milling at higher energy at an acceleration of 28 g in a new (MPL) mill produced damaged the silicon nitride particles, and should result in enhanced diffusivity during subsequent thermal processing. This high-energy milling produces only a small subtle increase in the crystal lattice parameters of the precursor components, but FTIR and solid-state MAS NMR spectroscopy suggest formation of new tetrahedral AlO_4 units and Si–O–Al bonds, possibly in solid solution or partially reacted hybrid particles. The replacement of alumina by AlN in the precursor mixtures is sufficient to maintain the necessary nitrogen content in the activated mixture.

Acknowledgements

Financial support by 6th FP under the project No. ACTIVATION NMP2-CT-2004-505885 is gratefully acknowledged. We are indebted to Dr. V. Kochnev's co-workers from TTD (St. Petersburg, Russia) for milling our specimens in his newly built MPL planetary mill. We truly appreciate all the fruitful discussions and advice from Galina Chernik and Nadezhda Budim (St. Petersburg University, Russia) on the mechanical activation of our powders.

References

1. Ekström, T. and Nygren, M., SiAlON ceramics. *J. Am. Ceram. Soc.*, 1992, **75**, 259–276.
2. Hayama, S., Nasu, T., Ozawa, M. and Suzuki, S., Mechanical properties and microstructure of reaction sintered β-sialon ceramics prepared by a slip casting method. *J. Mater. Sci.*, 1997, **32**, 4973–4977.
3. Suzuki, S., Nasu, T., Hayama, S. and Ozawa, M., Mechanical and thermal properties of β-sialon prepared by slip casting method. *J. Am. Ceram. Soc.*, 1996, **79**, 1685–1688.
4. Bulić, F. I., Zalite, N. and Zhilinska, N., Comparison of plasma-chemical synthesised SiAlON nano-powder and conventional prepared SiAlON powder. *J. Eur. Ceram. Soc.*, 2004, **24**, 3303–3306.
5. Zhang, D. L., Processing of advanced materials using high-energy mechanical milling. *Prog. Mater. Sci.*, 2004, **49**, 537–560.
6. Fecht, H. J., Nanostructure formation by mechanical activation. *Nanostructured Mater.*, 1995, **61**, 33–42.
7. Streletskii, A. N., Lapshin, V. I. and Fokina, E. L., Mechanical disordering of complex oxides with perowskite structure. *Kinetica i kataliz.*, 1989, **30**, 1064–1070.
8. Koch, C. C., Synthesis of nanostructured materials by mechanical milling. Problems and opportunities. *Nanostructured Mater.*, 1997, **9**, 13–22.
9. Temuujin, J., Okada, K. and MacKenzie, K. J. D., Formation of mullite from mechanochemically activated oxides and hydroxides. *J. Eur. Ceram. Soc.*, 1998, **18**, 831–835.
10. Heegn, H., Birkeneder, F. and Kamptner, A., Mechanical activation of precursors for nanocrystalline materials. *Cryst. Res. Technol.*, 2003, **38**, 7–20.
11. MacKenzie, K. J. D., Temuujin, J., Smith, M. E., Okada, K. and Kameshima, Y., Mechanochemical processing of sialon compositions. *J. Eur. Ceram. Soc.*, 2003, **23**, 1069–1082.
12. MacKenzie, K. J. D. and Barneveld, D. V., Carbothermal synthesis of β-sialon from mechanochemically activated precursors. *J. Eur. Ceram. Soc.*, 2006, **26**, 209–215.
13. Xu, X., Nishimura, T., Hirosaki, N., Xie, R.-J., Zhu, Y., Yamamoto, Y. and Tanaka, H., New strategies for preparing nanosized silicon nitride ceramics. *J. Am. Ceram. Soc.*, 2005, **88**(4), 934–937.
14. Xu, X., Nishimura, T., Hirosaki, T., Xie, R. J., Yamamoto, Y. and Tanaka, H., Fabrication of β-sialon nanoceramics by high-energy mechanical milling and spark plasma sintering. *Nanotechnology*, 2005, **16**(9), 1569–1573.
15. Antsiferov, V. N., Gilyov, V. G. and Karmanov, V. I., IR-spectra and phases structure of sialons. *Vibrat. Spectr.*, 2002, **30**, 169–173.
16. Chandradass, J. and Balasubramanian, M., Sol–gel processing of alumina-zirconia minispheres. *Ceram. Int.*, 2005, **31**, 743–748.
17. Cheng, H., Sun, Y., Zhang, J. X., Zhang, Y. B., Yuan, S. and Hing, P., AlN films deposited under various nitrogen concentrations by RF reactive sputtering. *J. Cryst. Growth*, 2003, **254**, 46–54.
18. Tseng, T. Y., Lin, C. C. and Liaw, J. T., Phase transformation of gel-derived magnesia partially stabilized zirconia. *J. Mater. Sci.*, 1987, **22**, 965–972.
19. Low, M. and McPherson, R., Crystallization of gel-derived alumina and alumina-zirconia ceramics. *J. Mater. Sci.*, 1989, **24**, 892–898.

20. Hess, P. and Lambers, J., Infrared spectra of photochemically grown sub-oxides and oxynitrides at the Si/SiO_2 interface. *Microelectr. Eng.*, 2004, **72**, 201–206.
21. Colomban, Ph., Structure of oxide gels and glasses by infrared and Raman scattering. *J. Mater. Sci.*, 1989, **24**, 3002–3010.
22. MacKenzie, K. J. D. and Smith, M. E., *Multinuclear Solid State NMR of Inorganic Materials. Pergamon Materials Series*, *vol. 6*. Pergamon/Elsevier, Oxford, 2002, pp. 247, 316.
23. Temuujin, J., Jadambaa, T. S., Okada, K. and MacKenzie, K. J. D., Preparation of aluminosilicate precursor by mechanochemical method from gibbsite-fumed silica mixtures. *Bull. Mater. Sci.*, 1998, **21**, 185–187.
24. Temuujin, J., Okada, K., MacKenzie, K. J. D. and Amgalan, J., Comparative study of mechanochemical preparation of aluminosilicate precursors from various aluminium hydroxides and amorphous silica. *Br. Ceram. Trans.*, 2000, **99**, 23–25.